

Implications of experimental probes of the RG-flow in quantum Hall systems

C.A. Lütken¹ and G.G. Ross²

¹*Theory Group, Department of Physics, University of Oslo*

²*Rudolf Peierls Centre for Theoretical Physics, Department of Physics, University of Oxford*

(Dated: May 15, 2022)

We review the implications of the scaling data for the emergent symmetry of the quantum Hall system. The location of the fixed points in the conductivity plane is consistent with the global, non-Abelian discrete symmetry $\Gamma_0(2)$, and the renormalisation group (RG) flow-lines agrees closely with that found if the symmetry acts anti-holomorphically. We extend the analysis to consider the rate of the RG flow. For a specific model in which the $\Gamma_0(2)$ symmetry acts anti-holomorphically the scaling close to the fixed points gives a critical delocalisation exponent $\nu = 2.38 \pm 0.02$, in excellent agreement with direct measurements and with numerical simulations. Both the predicted flow-lines and the flow rate also agree with the experimental measurements far away from the critical points, suggesting an emergent topological structure capable of stabilising the symmetry predictions. We hope that this agreement will stimulate further experimental study capable of conclusively testing the symmetry and exploring its associated dynamics.

PACS numbers: 73.20.-r

INTRODUCTION

The physics governing the plateaux transitions observed in the quantum Hall system is still poorly understood despite more than two decades of experimental and theoretical investigations. The transitions display a universal scaling behaviour and the identification of their universality class is an important part of our attempt to understand the quantum Hall system as it should reveal what the emergent symmetries and effective degrees of freedom of the system are, without which no deep understanding of the physics of this system can be claimed.

In this paper we look again at the wealth of experimental data on temperature driven flows both near and far from the critical points. From these data we will try to determine the global (geometrical and topological) and local properties of the RG flow in the effective field theory (EFT) of a strongly interacting spin-polarized two-dimensional electron gas. We will argue that these properties strongly suggests that the quantum Hall system possesses a beautiful emergent symmetry called $\Gamma_0(2)$, and that this symmetry in turn leads to a prediction for the effective dynamics of the system.

It has long been known that the RG fixed points of the (odd fraction and integer) quantum Hall system are related by the global discrete symmetry $\Gamma_0(2)$ [1]. This includes the stable fixed points (plateaux) where we have a reasonable understanding of the microscopic nature of the system due to work by R. Laughlin and others, but the symmetry applies over a much greater domain of the $(\sigma^{xy}, \sigma^{xx})$ conductivity plane. This includes the quantum critical points where the subtle and ill-understood delocalisation of the charge carriers (presumably anyons) takes place.

Furthermore, universal scaling behaviour follows if the

renormalisation group (RG) flow respects the symmetry away from the fixed points. The critical exponents obtained from the analysis of scaling data and from numerical simulations suggests that the RG flow is hyperbolic near critical points, i.e. the relevant and irrelevant exponents have the same absolute value. This in turn suggests that the symmetry acts anti-holomorphically near the fixed points [2]. As has been emphasised before [3, 4] the agreement of the $\Gamma_0(2)$ anti-holomorphic RG flow lines with the observed RG flow is impressive, both near and far from the critical points, cf. Fig.1.

The geometrical form of the RG flow-lines is only part of the story, as the rate of flow along these lines also provides important information. Most effort to date has been devoted to exploring the behaviour in the neighbourhood of the fixed points in order to determine the critical exponents. Experiments directly determining the exponent find a universal value $\nu_{\text{exp}} = 2.3 \pm 0.1$ [5], and $\nu_{\text{exp}} \approx 2.38$ [6, 7]. This is consistent with numerical studies [8, 9].

In a previous paper we determined the geometric exponent $\mu \approx 2.60512$ in a $\Gamma_0(2)$ -symmetric toroidal model [10]. In this paper we show that by taking into account the non-linear corrections evident in the scaling data the geometric exponent corresponds to a delocalisation exponent $\nu_{\text{tor}} = 2.38 \pm 0.02$, which is in excellent agreement with both the experimental and the numerical values. This is strong evidence that the toroidal model is in the same universality class as the quantum Hall system.

One can do more and use the toroidal model to determine the rates of flow far from the delocalisation fixed points, and we present a comparison of these flow rates with the available data. While the agreement is encouraging, further experiments are needed to test the model in detail. That the flow-lines and the flow rates should agree with the data far from the fixed points is remark-

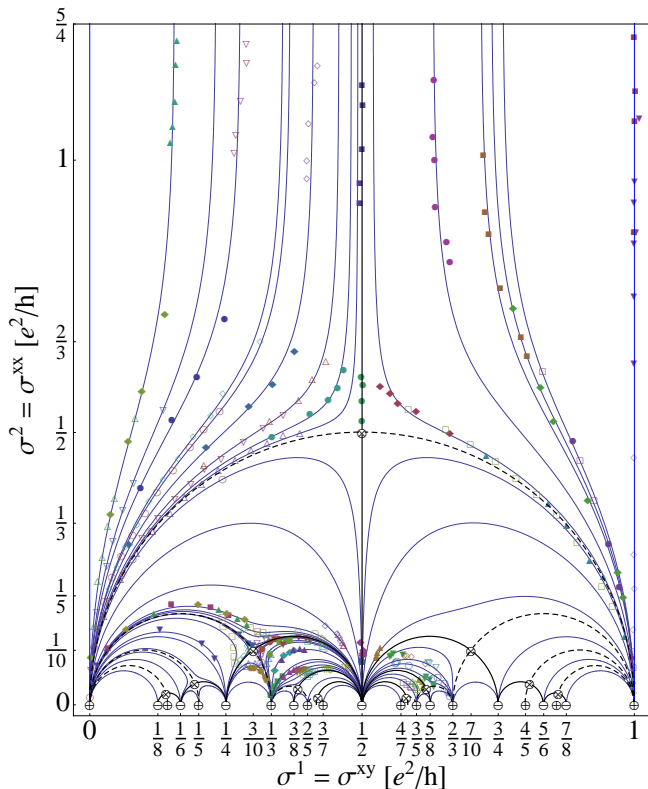


Figure 1: Compilation of temperature-driven flow data [3, 4] superimposed on RG flow-lines derived from the RG potential φ_H . Thick black lines are phase boundaries. Dashed lines are separatrices for the flow. The busiest region is shown under successive magnifications in Fig. 2 and Fig. 3.

able and requires an explanation. In our opinion it suggests that there must be some topological structure governing the quantum Hall system that is stable throughout the conductivity plane.

SCALING

We first introduce some notation relevant to the discussion of renormalisation group scaling in the quantum Hall system. As mentioned above the observed scaling behaviour is consistent with hyperbolic scaling near the delocalisation critical points and to describe this behaviour it is convenient to introduce complex coordinates to describe the $(\sigma^{xy}, \sigma^{xx})$ conductivity plane. Choosing $z := \sigma^1 + i\sigma^2$ and $\bar{z} := \sigma^1 - i\sigma^2$, where $\sigma^1 := \sigma^{xy}$ and $\sigma^2 := \sigma^{xx}$, the corresponding differentials are $\partial := \partial_z := (\partial_1 - i\partial_2)/2$ and $\bar{\partial} := (\partial_1 + i\partial_2)/2$, where $\partial_i := \partial/\partial\sigma^i$ ($i = 1, 2$) ($\partial_1 = \partial + \bar{\partial}$, $\partial_2 = i(\partial - \bar{\partial})$). Let ξ be the dominant scale parameter that, depending on the values of the control parameters (magnetic field, doping, etc.), could be temperature, inelastic scattering length, the size of the sample, etc. We have two real-valued

beta-functions, defined as usual by $\beta^i := \dot{\sigma}^i := d\sigma^i/dt$ ($i = 1, 2$), where $t = \ln(\xi/\xi_0)$, or equivalently the complex vector fields $\beta^z := \beta^1 + i\beta^2 = \dot{\sigma}^1 + i\dot{\sigma}^2 = \dot{z}$ and $\beta^{\bar{z}} := \beta^1 - i\beta^2 = \dot{\sigma}^1 - i\dot{\sigma}^2 = \dot{\bar{z}}$.

To discuss the general RG flow we also need local coordinates near each fixed point: $x + iy := z - z_*$ (i.e. $x(t) = \sigma^1(t) - \sigma_*^1$ and $y(t) = \sigma^2(t) - \sigma_*^2$). The beta-functions are unchanged by this change of coordinates: $\beta^1 = \dot{x} = dx/dt$, $\beta^2 = \dot{y} = dy/dt$, $\beta^z = \dot{x} + i\dot{y}$ and $\beta^{\bar{z}} = \dot{x} - i\dot{y}$.

We start the scaling flow when $t = 0$ at some initial point $z_0 := z(0)$ in parameter space, and first study the RG-flow in the scaling domain (very near a fixed point, i.e. $z_0 \approx z_*$) where the flow equations may be linearized:

$$\dot{\sigma}^i \approx \gamma_i(\sigma^i - \sigma_*^i) \quad (i = 1, 2). \quad (1)$$

The geometric critical exponents

$$\mu_i := 1/\gamma_i \quad (2)$$

parametrize the *geometric* flow rates near the fixed point. Without further constraints the flow does not enjoy any special analyticity properties:

$$z(t) = z_* + \Re(z_0 - z_*)e^{\gamma_1 t} + i\Im(z_0 - z_*)e^{\gamma_2 t},$$

and a more illuminating form of this equation is $y \propto x^c$ where $c := \mu_1/\mu_2$. The flow is holomorphic if $\gamma_1 = \gamma_2 := \gamma_*$, in which case we have:

$$\beta^z = \dot{z} \approx \gamma_*(z - z_*) \implies z(t) = z_* + (z_0 - z_*)e^{\gamma_* t}.$$

This may describe the flow near the UV- or IR-stable fixed points, which are either rational, $z_* = \sigma_*^{xy} \in \mathbf{Q}$, or the point at imaginary infinity, $z_\infty := i \lim(\sigma^{xx} \rightarrow \infty)$. Near these points (which compactify the upper half plane) the topology of the phase diagram forces the flow to be vertical, so that there indeed is only one exponent. If the exponent is negative, $0 > \gamma_* =: \gamma_\oplus$ (positive, $0 < \gamma_* =: \gamma_\ominus$) the fixed point $z_* =: z_\oplus$ ($z_* =: z_\ominus$) is attractive (repulsive).

If we demand that the fixed point be a saddle point, which means that one direction is attractive (contracting flow; $\gamma_2 < 0$) and one is repulsive (expanding flow; $\gamma_1 > 0$), then the exponents have opposite sign and the flow is given by $y \propto 1/x^{|\gamma_\oplus|}$. If the exponents also have the same absolute value ($\gamma_\otimes := \gamma_1 = -\gamma_2$) the flow is *hyperbolic*: $y \propto 1/x$. In this case we shall also refer to the flow as “anti-holomorphic” because $\beta^{\bar{z}} = \dot{\bar{z}} \approx \gamma_\otimes(\bar{z} - \bar{z}_\otimes)$.

$\Gamma_0(2)$ anti-holomorphic flow

The group $\Gamma_0(2)$ acts on the complex coordinate z and is generated by a translation $T : z \rightarrow z + 1$ and by the combination ST^2S where $S : z \rightarrow -1/z$ is a complexified

duality transformation. As originally noted in [1] the location of the fixed points associated with the integer and odd fractional quantum Hall states are consistent with a $\Gamma_0(2)$ symmetric RG flow. Superuniversality of the scaling exponents associated with the delocalisation fixed points follows automatically from this symmetry.

In the neighbourhood of the delocalisation fixed points the flow is found experimentally to be hyperbolic, i.e. anti-holomorphic [2]. In general it need not be anti-holomorphic at higher order, but if it happens to be a *globally* anti-holomorphic flow which also respects $\Gamma_0(2)$ (i.e., for which β_z is a weight-2 automorphic form), then it is given uniquely [10] (up to a constant) by the modular discriminant function Δ : $\beta_z \propto E_2(z) := \partial_z \varphi_H$, where

$$\varphi_H := \frac{1}{2\pi i} \ln \frac{\Delta(2z)}{\Delta(z)}. \quad (3)$$

A practical form of $E_2(z)$ useful for numerical work is given by the rapidly converging series expansion:

$$E_2(z) = 1 + 24 \sum_{n=1}^{\infty} \frac{nq^n}{1+q^n}, \quad (4)$$

where $q := \exp(2\pi iz)$.

In what follows we shall explore the hypothesis that this remarkable automorphic function contains all the universal information about the quantum Hall system, including global discrete symmetries, the existence and location of all RG fixed points (plateaux and delocalization fixed points), the critical exponents, the phase diagram, scaling laws, semi-circle laws, resistivity rules, etc [10].

THE GEOMETRY OF THE QUANTUM HALL RG FLOW

We turn now to a comparison of the $\Gamma_0(2)$ holomorphic flow with data. We start by comparing the geometry of the predicted RG flow-lines with data, ignoring for the moment the flow-rate.

Fig.1 shows a compilation of temperature-driven flow data [3, 4] superimposed on RG flow-lines derived from the RG potential φ_H defined in eq.(3). Thick black lines are phase boundaries. Dashed lines are separatrices for the flow and have the characteristic form of semi-circles (“the semi-circle rule”). The busiest region is shown under successive magnifications in Fig.2 and Fig.3. The integer data were obtained for temperatures ranging over two decades, from 4.2 K down to 40 mK, for a variety of samples and magnetic fields [3]. The diagram has been rescaled by 0.5 to remove the effect of having two flavors of charge carriers (spin up and spin down), as explained in [3]. Data points for the flow in fractional phases were obtained for a single sample at temperatures $T = 0.3\text{K}, 0.2\text{K}, 0.11\text{K}, 0.06\text{K}, 0.035\text{K}$ [4].

Unfortunately errors are not estimated in these references. We have allowed for some small systematic errors in both sets of data, in order to align the experimental and theoretical separatrices. The experimental separatrix for the integer flow is centered about 1% below the point $(1/2, 0)$, so these data have been shifted up by 0.01. Similarly, the experimental separatrix for the fractional flow to the left of $\sigma^{xy} = 1/2$ appears to be slightly rotated, so these data have been rotated by 5.5 degrees around $(1/6, 0)$ in order to align the separatrices. This systematic error may be due to a macroscopic inhomogeneity in the sample [4].

The theoretical flow-lines were obtained by numerically integrating the RG equations:

$$\begin{aligned} \dot{x} &= \Re\{Ny^2 E_2(z)\} \\ \dot{y} &= -\Im\{Ny^2 E_2(z)\} \end{aligned} \quad (5)$$

where N is a normalisation constant and we have used the hyperbolic metric [10]. $E_2(z)$ is the holomorphic and automorphic form given in eq.(4), retaining 50 terms in the sum in order to get sufficient accuracy near the real line. We get to pick the starting point for each particular flow-line, but this completely fixes the geometry of the curve.

Given the lack of error estimates it is impossible to provide a quantitative estimate of the goodness of fit, but qualitatively the agreement of the $\Gamma_0(2)$ holomorphic flow geometry with the data is impressive and consistent over the range of parameter space explored so far.

THE RG FLOW RATE

Identification of the symmetry can lead to a detailed prediction of the effective dynamics governing the flow. The observation that the symmetry acts anti-holomorphically led us to identify a class of effective scaling models consistent with $\Gamma_0(2)$, which is parametrized by the complex structure of a torus with a special spin structure, in which only the number f of flavors of fermions remains undetermined [10]. Together with the hyperbolic metric used in eq.(5) these models allow us to determine the normalisation constant N as a function of f . Comparison with the data discussed below shows that a consistent picture emerges for $f = 2$, corresponding to $N \approx 0.2518i \approx i/4$, and these are the values used in the fits presented here.

To test the resulting prediction for the RG flow rate we must go beyond the comparison with the geometrical form of the flow-lines tested above. In particular, it is clear from eq.(5) that the gradient of the flow-line is independent of the metric and normalisation, and is determined by the $\Gamma_0(2)$ function $E_2(z)$ only. Testing the flow rate is crucial to a complete test of the RG form given in eq.(5).

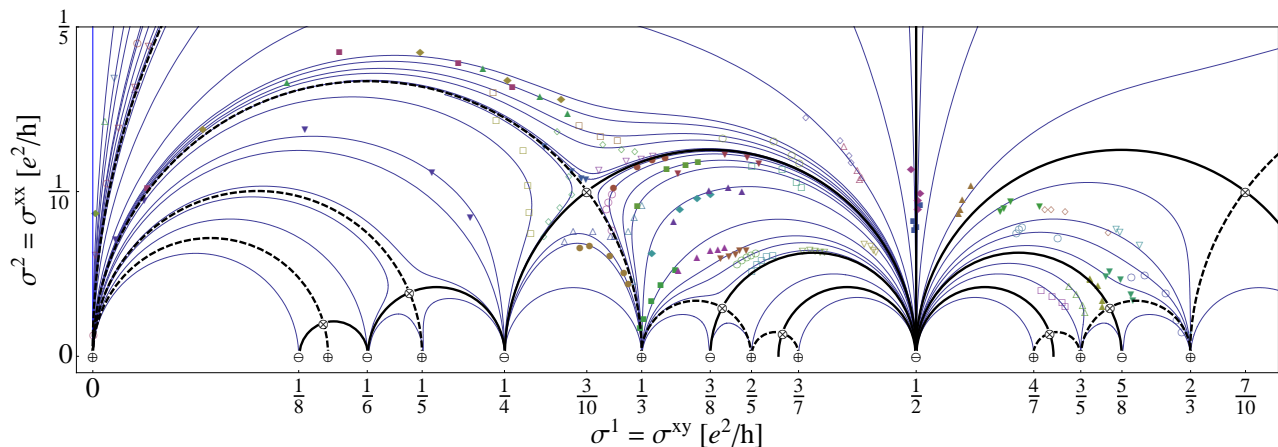


Figure 2: Comparison of experimental temperature-driven flow [4] with our theoretical model. The data with $\sigma^{xy} < 1/2$ have been rotated by 5.5 degrees around $(1/6, 0)$ in order to align the separatrices. This systematic error may be due to a macroscopic inhomogeneity in the sample [4].

We start with a general comparison of the predicted flow rates with the data over the whole conductivity plane; the data in the region close to the delocalisation fixed points is discussed in the next section. Fig.3 compares the experimental temperature-driven flows [4] with our theoretical model. We have equipped the experimental data points in this diagram with “fake” error bars in order to distinguish them clearly from the theoretical points derived from the toroidal model (the displayed error-bars correspond to errors of approx. 1% in σ^{xy} and 3% in σ^{xx}). The data appear to follow the shape of the theoretical flow-lines quite closely.

The bullets and circles indicate the theoretical flow rate if the standard scaling assumptions are made in order to relate the temperatures $T = 0.3\text{K}, 0.2\text{K}, 0.11\text{K}, 0.06\text{K}, 0.035\text{K}$ at which data were obtained, to the correlation lengths $\xi(T)$:

$$t(T) := \ln \xi(T) = p \ln(T_0/T)/2, \quad (6)$$

where p is the inelastic scattering-rate exponent, and $p \approx 3.4$ is chosen for best fit. As discussed below non-universal values for p may be expected for the GaAs-AlGaAs samples studied in [4]. The saddle point $\otimes = (3/10, 1/10)$ is the quantum critical point controlling the delocalization transition to the $\sigma^{xy} = 1/3$ phase. The fixed points $\oplus = (1/3, 0)$ and $\ominus = (1/4, 0)$ are attractive and repulsive, respectively. The thick black line is a phase boundary, while the dashed line is a separatrix of the flow.

The agreement is highly non-trivial, as it depends delicately on the choice of metric, the scaling relations and the global value of p . The agreement for the three highest temperatures (red/grey bullets: ~ 100 mK) is in most cases very good (usually within one “fake” sigma, i.e. perfect agreement). For the two lowest temperatures

(circles: ~ 10 mK) the agreement is less impressive; the theory points are indicated by red/grey and black circles for $T = 0.06\text{K}, 0.035\text{K}$, respectively. The theory appears to *systematically* underestimate the flow-rate in this regime, but notice that the theory is extremely sensitive to changes in T . For example, if the quoted temperatures are just 10 mK too high the agreement is much better: almost all points agree within two “fake” sigmas. Notice also that the hyperbolic metric plays an essential role. A very small change in the metric immediately destroys the agreement. Using a flat metric is completely ruled out.

Critical exponents

There have been several experiments performed in the neighbourhood of the delocalisation fixed points to determine the critical exponents. The starting point is the magnetic field dependence of the localisation length ξ of electron states in the centre of an impurity-broadened Landau Level, $\xi \propto |B - B_*|^{-\nu}$, where B is the magnetic field and B_* is the critical field strength [11].

The most direct method of measuring ν was developed by Koch *et al.* [5] using size dependent scaling. The experiment studies several Hall bars with various widths and determines the half-width ΔB of the ρ_{xx} peak between adjacent Hall plateaux at the point that the temperature driven flow saturates. This corresponds to the point at which the localisation length equals the bar width and hence the experiment directly measures the dependence of ξ on ΔB , from which ν can be determined. For transitions between integer quantum Hall states the experiment found a universal value $\nu_{\text{exp}} = 2.3 \pm 0.1$.

A less direct method uses temperature dependent scal-

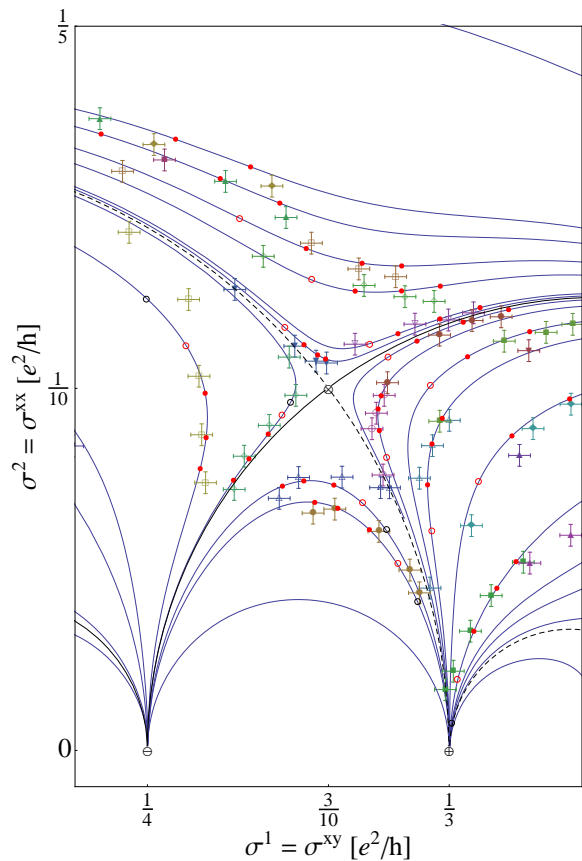


Figure 3: Comparison of experimental temperature-driven flows [4] with our theoretical model. The (red/grey) bullets and the (red/grey and black) circles are explained in the text.

ing. It measures the the half-width ΔB of the ρ_{xx} peak and the maximum slope of ρ_{xy} as a function of temperature. These have the scaling behaviour $\Delta B \propto T^\kappa$ and $(\partial\rho_{xy}/\partial(B - B_*))^\text{max} \propto T^{-\kappa}$, where the temperature exponent κ is related to the delocalisation critical exponent by $\kappa = p/2\nu$, and p is the temperature exponent of the inelastic scattering rate. The half-width is defined to be the width ΔB between the inflection points of $\rho^{xx}(B)$. The empirical fact that these points appear to coincide with the points of maximal curvature of $\rho^{xy}(B)$ is a consequence of the resistivity rule [12], and at least in the scaling domain we may therefore expect the two graphs to contain the same information.

Unfortunately the measurement of the critical exponent κ from temperature driven flows does not give the exponent ν directly, since the value of p must also be determined. For the samples studied by Koch *et al.* [5] non-universal values for p were found ranging from $p \approx 2.7$ to $p \approx 3.4$. Non-universality of the exponent κ was also found in [13].

Wei *et al.* [6] measured p in the integer quantum Hall effect by measuring the dependence of the effective tem-

perature of the electron gas on the applied current. They also obtained $\kappa \approx 0.42$ for the same sample and hence were able to provide an independent measurement of p and ν , finding $p \approx 2$ and $\nu_\text{exp} \approx 2.4$.

In a very recent study Wanli Li *et al.* [7] found perfect power-law scaling with $\kappa = 0.42 \pm 0.01$ over two decades of temperature, and measured $p \approx 2$ directly from a size dependent study, corresponding to $\nu_\text{exp} \approx 2.38$.

The observation of a universal value for κ in a subset of experiments has been explained in recent work by Wanli Li *et al.* [14]. They showed that universality applies to samples with short-range disorder such as $Al_xGa_{1-x}As/Al_{0.33}Ga_{0.67}As$ hetero-structures for x between 0.65% and 1.6%. Universality is not found in samples in which the disorder is dominated by long-range ionized impurity potentials.

Using variable-range hopping theory Hohls *et al.* [13] obtained $\nu_\text{exp} \approx 2.35$ directly from temperature driven flows.

Temperature dependent scaling has also been studied for the transition between the fractional quantum Hall states $2/5 \rightarrow 1/3$ [15]. A value of $\kappa \approx 0.42$ was also found for this case, but the value of p was not measured.

How do these measurements relate to the scaling properties of eq.(5)? Close to the delocalisation fixed point the RG flow is given by eq.(1) and the geometric exponents are defined in eq.(2). They are determined by the dependence of the localisation length on $\Delta\sigma$. Equivalently, for the conductivity range relevant to the Koch *et al.* experiment [5], one can determine it from the same dependence of the localisation length on the resistivity, $\Delta\rho$. On the other hand the delocalisation exponent is determined by the dependence of the localisation length on ΔB . To relate the two we need to determine the dependence of the resistivity on the magnetic field, which can be parameterised by the exponent α in $\Delta\rho \propto \Delta B^\alpha$. If $\alpha = 1$ then the geometric delocalization exponent is $\nu_\text{tor} = \mu \approx 5.210/f$ [10].

However, as may be seen from the inset in Fig.4, over the relevant range between inflection points there is a departure from linearity. To correct for this we determine α from the magneto-resistance data by a fit (see Fig.4) to the experimental ρ^{xy} -curves in [5] over the range of field values between the points of maximum curvature, which by the resistivity rule correspond to the inflection points of ρ^{xx} that are used to define the half-width. The “data points” in Fig.4 are a random but representative sample of resistivity values for $\Delta B = B - B_* > 0$, while the straight lines are least chi-square fits. Deviations from scaling appear far from the critical value ($\Delta B = 0$). Consistency is verified by the fact that these lines are parallel, with a mean slope of $\alpha = 0.913 \pm 0.008$.

Using this gives a geometric delocalization exponent $\nu_\text{tor} = \mu \times \alpha = 2.38 \pm 0.02$, where we have used the value $\mu \approx 2.605$ for the geometric exponent in the bi-

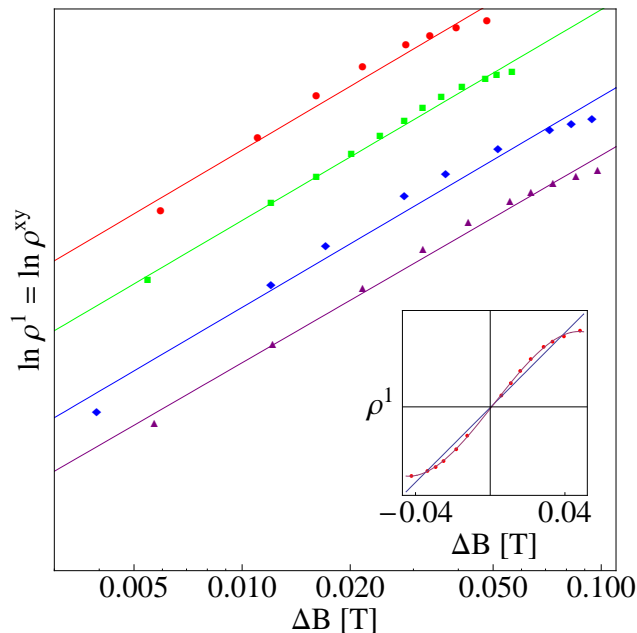


Figure 4: Non-linear corrections to naive scaling for the four Hall-bar geometries considered in [5] (triangles, diamonds, squares and bullets correspond to widths $w = 10, 18, 32$ and 64 microns, respectively). The inset shows some points on $\rho^1(\Delta B) = \rho^{xy}(\Delta B)$ between the points of maximum curvature, for $w = 64\mu m$, together with chi-square fits to a line and a cubic curve.

flavored ($f = 2$) toroidal model [10]. This is in excellent agreement with the experimental results described above ($\nu_{\text{exp}} = 2.3 \pm 0.1$ [5], 2.4 [6], 2.35 [13], 2.38 [7]), which appear to be converging on a value slightly below 2.4 , as well as the value $\nu_{\text{num}} = 2.35 \pm 0.03$ [9] obtained from numerical simulations of this quantum phase transition.

THE RESISTIVITY RULE AND CHARGE-FLUX DUALITY

In addition to the RG flow data discussed above there are several other measurements that suggest a connection of the quantum Hall system with the emergent $\Gamma_0(2)$ symmetry discussed here. An intriguing empirical observation [12] is the “resistivity rule” $d\rho^{xy}/d\log B \propto n\rho^{xx}$, where n is the carrier density. We have checked that this rule applies in the quantum regime studied in [5], where B (not ΔB) is approximately constant over the transition region. It is interesting to note that this connection between ρ^{xy} and ρ^{xx} follows along the $\Gamma_0(2)$ semi-circle separatrices of the RG flow connecting fixed points if one identifies the angular variable with ΔB , the applied magnetic field difference.

Another piece of evidence pointing to an emergent $\Gamma_0(2)$ symmetry is the longitudinal, non-linear, current-

voltage characteristics observed near the quantum Hall liquid to insulator transition. It is found [16] that the IV_{xx} -characteristics obtained on both sides of some transitions (from the quantum Hall liquids with filling factors 1 and $1/3$ into the neighboring insulator) map into each other under the duality transformations contained in the emergent $\Gamma_0(2)$ symmetry. The agreement is essentially perfect within the very small errors obtained in these impressive experiments (less than the pixel size in the plots), and probes the duality symmetry far away from the scaling domain close to the quantum critical points. It will be interesting to see whether the actual shapes of the IV_{xx} -curves can be obtained directly from the emergent symmetry.

DISCUSSION

In this paper we have reviewed the evidence coming from scaling data that the quantum Hall system involving integer and fractional odd denominator states has a non-Abelian discrete symmetry, $\Gamma_0(2)$. Numerical studies suggest that the RG flow is hyperbolic near critical points suggesting that the symmetry acts anti-holomorphically. This observation led us to identify a class of effective scaling models consistent with this symmetry, which is parametrized by the complex structure of a torus with a special spin structure, in which only the number of flavors of fermions remains undetermined [10].

Remarkably, not only do the positions of the fixed points and the RG flow-lines agree with the data, but the detailed flow rates also agree with the bi-flavored toroidal model, both close to and far away from the critical points. Why the agreement should persist far from the critical points is not known but strongly suggests that there is some topological order in the quantum Hall system [17].

While this agreement with data is very encouraging, in view of the experimental uncertainties it falls short of a definitive test of the theory based on the symmetry group $\Gamma_0(2)$. In particular, we would dearly like more experimental determinations of the critical exponents, particularly for the fractional quantum Hall system where a direct measurement of the delocalisation exponent has yet to be performed. This can be done by size-dependent scaling experiments, or by temperature dependent scaling experiments which directly measure the localisation length. As we have stressed repeatedly here, it is also important to test theory away from the critical points since this may confirm that a new topological structure is playing a role in the quantum Hall system.

[1] C.A. Lütken, G.G. Ross, Phys. Rev. B **45**, 11837 (1992); **48**, 2500 (1993); C.A. Lütken, J. Phys. A **26**, L811

- (1993); Nucl. Phys. B **396**, 670 (1993)
- [2] C.A. Lütken, G.G. Ross, Phys. Lett. A **356**, 382 (2006)
- [3] S.S. Murzin, M. Weiss, A.G.M. Jansen, K. Eberl, Phys. Rev. B **66**, 233314 (2002)
- [4] S.S. Murzin, S.I. Dorozhkin, D.K. Maude, A.G.M. Jansen, Phys. Rev. B **72**, 195317 (2005)
- [5] S. Koch, R.J. Haug, K.v. Klitzing, K. Ploog, Phys. Rev. Lett. **67**, 883 (1991); Phys. Rev. B **46**, 1596 (1992)
- [6] H.P. Wei, L.W. Engel, D.C. Tsui, Phys. Rev. B **50**, 14609 (1994)
- [7] Wanli Li, C.L. Vicente, J.S. Xia, W. Pan, D.C. Tsui, L.N. Pfeiffer, K.W. West, Phys. Rev. Lett. **102**, 216811 (2009)
- [8] J.T. Chalker, P.D. Coddington, J. Phys. C **21**, 2665 (1988); B. Huckestein, B. Kramer, Phys. Rev. Lett. **64**, 1437 (1990); D.-H. Lee, Z. Wang, S. Kivelson, Phys. Rev. Lett. **70**, 4130 (1993); J.T. Chalker, J.P.G. Eastmond, as reported in B. Huckestein, Rev. Mod. Phys. **67**, 357 (1995)
- [9] B. Huckestein, Europhys. Lett. **20**, 451 (1992); Phys. Rev. Lett. **72**, 1080 (1994)
- [10] C.A. Lütken, G.G. Ross, Phys. Lett. B **653**, 363 (2007)
- [11] A. Pruisken, in *The Quantum Hall Effect* (Springer-Verlag, 1990), eds. R.E. Prange and S.M. Girvin
- [12] A.M. Chang, D.C. Tsui, Solid State Commun. **56**, 153 (1985); H.L. Störmer, K.W. Baldwin, L.N. Pfeiffer, K.W. West, Solid State Commun. **84**, 95 (1992); T. Rötger, G.J.C.L. Bruls, J.C. Maan, P. Wyder, K. Ploog, G. Wiemann, Phys. Rev. Lett. **62**, 90 (1989)
- [13] F. Hohls, U. Zeiter, R.J. Haug, Phys. Rev. Lett. **88**, 036802 (2002)
- [14] Wanli Li, G.A. Csathy, D.C. Tsui, L.N. Pfeiffer, K.W. West, Appl. Phys. Lett. **83**, 2832 (2003); Phys. Rev. Lett. **94**, 206807 (2005)
- [15] L.W. Engel, H.P. Wei, D.C. Tsui, M. Shayegan, Surface Science **229**, 13 (1990)
- [16] D. Shahar, D.C. Tsui, M. Shayegan, R.N. Bhatt, J.E. Cunningham, Phys. Rev. Lett. **74**, 4511 (1995); L.W. Wong, H.W. Jiang, N. Trivedi, E. Palm, Phys. Rev. B **51**, 18033 (1995); D. Shahar, D.C. Tsui, M. Shayegan, E. Shimshoni, S.L. Sondhi, Science **274**, 589 (1996); E. Shimshoni, S.L. Sondhi, D. Shahar, Phys. Rev. B **55**, 13730 (1997)
- [17] C.A. Lütken, G.G. Ross, work in progress